ORIGINAL PAPER   **Open Access**

Experimental investigation on a novel approach for laser surface hardening modelling

L. Orazi[1,2*], A. Rota[3,4] and B. Reggiani[1,4]

Abstract

Laser surface hardening is rapidly growing in industrial applications due to its high flexibility, accuracy, cleanness and energy efficiency. However, the experimental process optimization can be a tricky task due to the number of involved parameters, thus suggesting for alternative approaches such as reliable numerical simulations. Conventional laser hardening models compute the achieved hardness on the basis of microstructure predictions due to carbon diffusion during the process heat thermal cycle. Nevertheless, this approach is very time consuming and not allows to simulate real complex products during laser treatments. To overcome this limitation, a novel simplified approach for laser surface hardening modelling is presented and discussed. The basic assumption consists in neglecting the austenite homogenization due to the short time and the insufficient carbon diffusion during the heating phase of the process. In the present work, this assumption is experimentally verified through nano-hardness measurements on C45 carbon steel samples both laser and oven treated by means of atomic force microscopy (AFM) technique.

Keywords: Laser hardening, Carbon diffusion, Austenite homogenization, AFM, Numerical model, Carbon steels

Introduction

Laser hardening is a surface process with some peculiar characteristics such as that it does not require a quenching medium and it can be more selective if compared to the classical treatments carried out in an oven or by induction hardening. Furthermore, concave features like gear teeth root and caves are more easily processed compared to induction technique, and different shapes do not require the manufacturing of new customized induction wires. With the use of high-efficiency diode laser (Ion 2002), also the overall efficiency of the process could be sensibly higher than induction hardening that,

given the lower power density, normally requires applied power of many teens of kW (Mühl et al. 2020). A detailed and up-to-date review about the process can be found in (Babu and Marimuthu 2019).

The effective applicability of laser transformation hardening depends on two basic aspects that determine the most important challenges in the development of this manufacturing technology: an accurate determination and control of the thermal field occurring onto the workpiece and the optimization of the laser scanning strategy when the part surface is larger than the beam spot size and thus multiple tracks have to be carried out (Tani et al. 2008). Concerning the first aspect, due to the fast heat cycle occurring when the laser beam irradiates the target material, the hysteresis in the austenization of the steel is very high and the actual transformation occurs at temperatures very near to the solidus one. This consideration leads to conclude that an inaccurate control of the surface temperature can easily determine the

* Correspondence: leonardo.orazi@unimore.it
[1]DISMI - Department of Sciences and Methods for Engineering, University of Modena and Reggio Emilia, Reggio Emilia, Italy
[2]EN&TEC - Centro Interdipartimentale per la Ricerca Industriale ed il Trasferimento Tecnologico nel Settore delle Tecnologie Integrate per la Ricerca Sostenibile, della Conversione Efficiente dell'Energia, l'Efficienza Energetica degli Edifici, l'Illuminazione e la Domotica, University of Modena and Reggio Emilia, Reggio Emilia, Italy
Full list of author information is available at the end of the article

partial melting of the target material and consequently the inevitable impairment of the workpiece quality. Concerning the second aspect, the matter is probably even more serious: if the surface to be hardened is large and a single track is not sufficient to cover it, several adjacent tracks have to be performed determining an inevitable tempering of the previously hardened material due to its interaction with the thermal field caused by the later tracks. On the basis of the abovementioned considerations, setting up an effective laser surface hardening treatment emerges to be a complex activity often involving a costly and time expensive trial-and-error approach.

A possible approach to estimate the outcome of the laser hardening process is through the use of design of experiment techniques that permit to generate models correlating operating parameters with hardened thickness and/or hardened width. Examples applied to low-carbon steels can be found in (Babu et al. 2013; Chen et al. 2020).

Another approach is based on the numerical simulation of the phenomena involved in the process in order to allow a deep understanding of the process mechanisms while reducing and minimizing the experimental activities.

Many researchers stressed on the importance of laser hardening process simulation and many different modelling approaches were proposed in the last couple of decades. Theoretically, the process simulation requires the prediction of the thermal field in the target part, of the austenite formation, carbon diffusion and austenite homogenization and, finally, the microstructure prediction during the cooling. The thermal field can be predicted by solving the Fourier equation in the target domain, while, more attention needs the austenite formation prediction. The canonical model for the austenization of hypo-eutectoid steels in quasi-static conditions considers two distinct processes: the perlitic colony and ferritic grains transformations, due to the change from BCC to FCC of the iron lattice, and the homogenization of the obtained austenitic grains. These two processes are both considered in determining the set up for the proper conduction of the heat treatments in an oven. One of the first simulation model for the laser hardening can be found in (Ashby and Easterling 1984; Li et al. 1986), and it is based on a microstructural approach according to the heat treatments in an oven. This approach was then applied by other authors as in (Ohmura and Inoue 1989) in which it is supposed that the pearlite to austenite transformation terminates at the AC_3 temperature for a pure iron considering a fixed and very high heating rate.

The availability of new, simple, reliable and efficient diode laser sources is probably the key factor that pushed several authors to reinvestigate laser surface hardening in the last years: the works in (Skvarenina and Shin 2006; Patwa and Shin 2006) are all based on the same microstructural approach presented in (Ashby and Easterling 1984; Li et al. 1986) and on the hypotheses formulated in (Jacot and Rappaz 1997; Jacot and Rappaz 1998). Another model based on a commercial Finite Element Method software was presented in (Miokovic et al. 2006; Miokovic et al. 2007).

In all the cited works, a heat conduction model with non-constant parameters is coupled with a phase transformation model evaluated at the microscale. All those approaches predict both the resulting phases and the hardness at the cost of a very long calculation time: the time step that guarantees the stability of the numerical integration is inversely proportional to the absolute values of the diffusivity and to the grid dimension and both of them are very small when applied to the microstructure in solid phases as shown in Eq. (1) where ρ is the density in $\frac{kg}{m^3}$, c_p is the specific heat in $\frac{J}{kg\,K}$, κ the material conductivity in $\frac{W}{m\,K}$ and Δx, Δy and Δz are the dimensions of the 3D cell calculation.

$$\Delta t \leq \frac{1}{2}\frac{\rho\,c_p}{k}\frac{1}{\left(\frac{1}{\Delta x^2}+\frac{1}{\Delta y^2}+\frac{1}{\Delta z^2}\right)} \tag{1}$$

Small Δt and consequently long calculation time makes these models useless to simulate real complex applications, such as multi passes processes on real 3D objects.

An attempt to overcome these limitations was previously presented by the authors by introducing the hypothesis that carbon diffusion can be neglected during the austenization in the modelling of laser surface hardening process of hypo-eutectoid steels due the short time and the insufficient carbon diffusion during the heating phase of the process (Orazi et al. 2010). In more detail, it was shown that the accuracy in the hardness prediction as achieved by the numerical model remains high but the calculation time can be sensibly reduced and a real process optimization can be carried out in industrial components (Tani et al. 2010). However, in the aforementioned contributions, the neglecting of the austenite homogenization (carbon diffusion) was assumed as starting hypothesis however without any specific experimental validation. In the present work, experiments are presented to prove that austenite homogenization in laser surface hardening does not take place and it can be therefore neglected in process modelling and optimization. To this aim, a novel indirect approach to evaluate carbon diffusion during laser hardening and conventional oven hardening is used and discussed based on hardness measurements obtained by means of atomic force microscopy (AFM) technique applied on

specimens made of C45 EN 10277-2 steel whose chemical composition is reported in Table 1.

The novel approach
From a physical point of view, the laser hardening process differs from the oven process for some important aspects:

- The quenching (cooling) is performed by conduction in the bulk volume.
- The process is very fast: fraction of seconds compared to fraction of hours.
- Heating and cooling rate are very high.
- Solid phase transformations happen with significant over and under heating due to the process hysteresis.

According to all these reasons, during laser surface hardening of thick, bulk parts with high thermal inertial almost all the austenized material become martensite after cooling and attention can be focused in obtaining austenite during the heating stage.

In (Jacot and Rappaz 1997; Jacot and Rappaz 1998), it is clearly demonstrated that, in case of high overheating, as in the laser hardening process, the carbide diffusion in the austenite mainly happens in the lateral side of the carbide plates as in Fig. 1, leading to a change in the cross-section of the carbon flux from λL as (Ashby and Easterling 1984; Li et al. 1986) to L^2, where L is the characteristic size of the perlite colony, having order of several μm, and λ is the thickness of the lamina that is normally a fraction of μm.

Following this track, authors proposed in (Orazi et al. 2010), successively extended in (Fortunato et al. 2013), a model to simulate the effect of laser surface hardening process in terms of achieved hardness and microstructure. An integral transformation parameter $I_{p \to a}$ has been introduced and expressed in Eq. (2):

$$I_{p \to a} = \int_{t_{A_{c1}}}^{t_{A_{r1}}} \exp\left(-\frac{Q_{p \to a}}{RT(t)}\right) dt \qquad (2)$$

in which t is the time in s, Q is the activation energy in J, R the gas constant in $\frac{J}{K}$, T the temperature of the material in K, $t_{A_{c1}}$ is the time at which the steel overcome temperature A_{c1} and $t_{A_{r1}}$ is the moment when it descends below A_{r1}. In the proposed model, it is

supposed that austenization completes when the value of the parameter $I_{p \to a}$ overcomes a threshold, $I_{p \to a, th}$, experimentally determined.

$$I_{p \to a} \geq I_{p \to a, th} \qquad (3)$$

The previous model is based on the hypothesis that, due to the short interaction time in laser hardening, carbon diffusion can be neglected and no homogenization occurs in the austenitic grains. According to this new process simulation frame, laser surface hardening can be modelled in the following 3 steps:

1. Thermal field evaluation into the working part according to the laser parameters and scanning strategies.
2. Evaluation of Eq. (2) into the working part.
3. Declare austenite and consequently martensite formation where Eq. (3) is verified.

The different approaches between the traditional process modelling, based on the microstructure prediction, and the proposed new one is presented in Fig. 2.

As previously stated, the present work was aimed at verifying the assumption of austenite homogenization according to the carbon diffusivity at the high temperature achieved during laser hardening process. However, if it is easy to experimentally observe or calculate that during laser hardening the temperature, in the proximity of the surface, can be very close to the melting temperature, unfortunately, there are not so many information about carbon diffusivity in these extreme conditions. A brief state of the art on this aspect is then presented in the next section with the aim to introduce the novel adopted experimental approach.
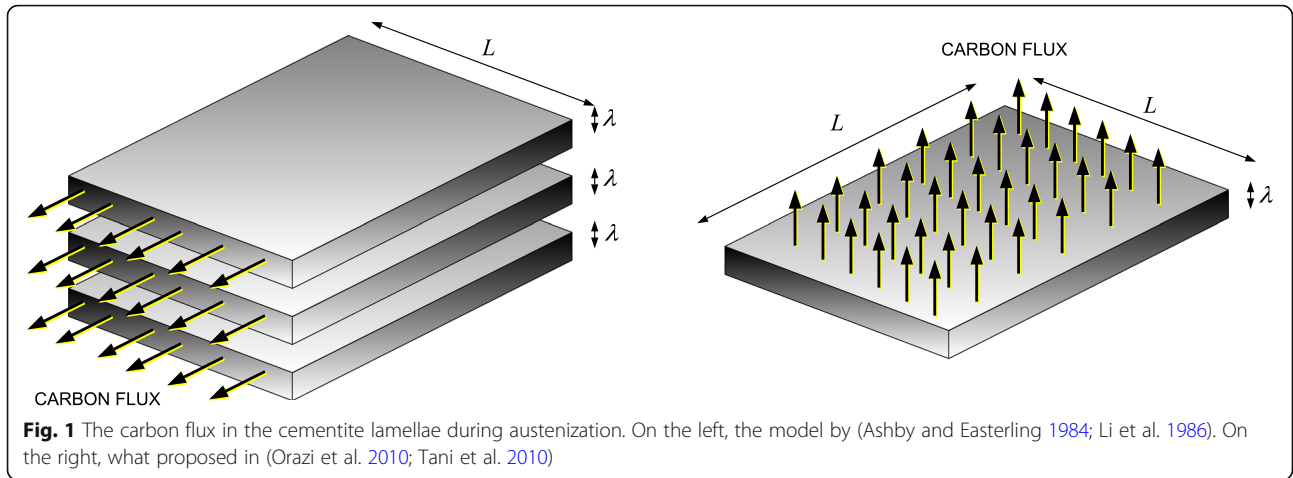
Evaluation of carbon diffusivity
First historical measurements on carbon diffusivity at high temperature were done in (Weels and Mehl 1940; Weels et al. 1950), in which several tests by coupling steel disks with different carbon concentration and annealing at temperature between 750 and 1305 °C were executed.

In (Tibbetts 1980), different tests of plasma carburizing were performed in order to measure carbon diffusivity at high temperature for ferrous alloys. The author used the steady-state method previously applied by (Smith 1953) at ambient temperature.

In (Bhadesia 1981), the author used data from the previous works in order to obtain a more accurate estimation of the diffusivity that is nevertheless only expressed in graphical form.
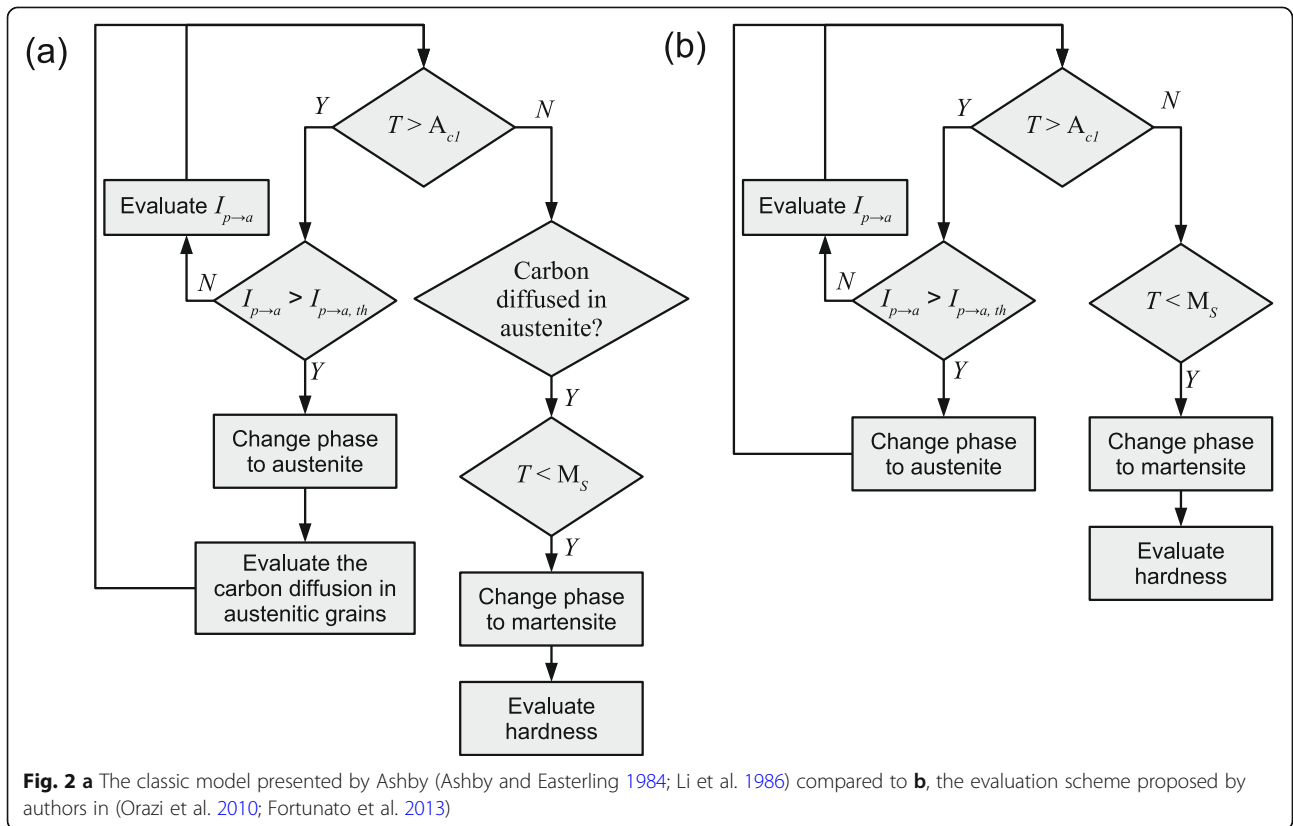
Table 1 Chemical composition of C45 steel

C %	Si %	Mn %	P %	S %	Cr %	Ni %	Mo %
0.42–0.50	< 0.4%	0.50–0.80	< 0.045	< 0.045	< 0.4	< 0.4	< 0.1

Fig. 1 The carbon flux in the cementite lamellae during austenization. On the left, the model by (Ashby and Easterling 1984; Li et al. 1986). On the right, what proposed in (Orazi et al. 2010; Tani et al. 2010)

In (Karabelchtchikova and Sisson Jr 2006), an estimation of the carbon diffusivity in austenite during gas carburizing is obtained by fitting a numerical model of the carbon diffusivity with the surface carbon content at different process parameters. With this approach, the diffusivity appears to range between $1.68 \cdot 10^{-7}$ cm^2/s at 880 °C and $5.06 \cdot 10^{-8}$ cm^2/s at 980 °C.

In (Lee et al. 2011), a critical review of twelve models for the carbon diffusivity in austenite is performed by evaluating their fitting with different sets of experimental data collected from literature. As expected, the models that generate the best numerical-experimental agreement were those including the influence on the diffusivity of the carbon content, the temperature and the alloying elements both on the diffusivity coefficient D and on the activation energy Q. The best equation obtained from the whole dataset is reported in Eq. (2):

Fig. 2 a The classic model presented by Ashby (Ashby and Easterling 1984; Li et al. 1986) compared to **b**, the evaluation scheme proposed by authors in (Orazi et al. 2010; Fortunato et al. 2013)

$$D(T, C) = (0.146 - 0.036C)$$
$$\cdot \exp\left(-\frac{144.3 - 15.0C + 0.37C^2}{R}\right) \quad (4)$$

where D is the carbon diffusivity in cm^2/s, C the carbon content in mass percentage, T the temperature in °K, and R is the gas constant. As an example, a plot of the model as applied to C45 with a carbon content of 0.45% is reported in Fig. 3.

The reported carbon diffusivity models proposed in (Karabelchtchikova and Sisson Jr 2006; Lee et al. 2011) are used as references to estimate the carbon diffusion length l_c given by Eq. (5):

$$l_c = \sqrt{D\,\tau} \quad (5)$$

where D is the diffusivity and τ the time spent at a given temperature. Table 2 shows the diffusion length $l_c(1s)$ calculated at 1 s of interaction.

As can be seen, some discrepancy between data from different sources are present but the diffusion length $l_c(1\ s)$ appears quite small compared to the average size of perlite colonies. This substantially confirms the hypothesis underlying the model proposed in (Orazi et al. 2010; Fortunato et al. 2013), but it also suggests how difficult is to obtain reliable data about carbon diffusivity at high temperature,

For these reasons, in the present work, it is proposed to evaluate the homogeneity of the carbon into the structure by an indirect experimental method consisting in the post hardening microstructure analysis via nano indentations. As already reported in literature (Furuhara et al. 2003), the hardness increasing in metallurgic tempering processes are related to intra-granular carbon diffusion in the pearlitic structures and inter-granular carbon diffusion between pearlitic and ferritic grains. To identify these mechanisms and to relate them to carbon
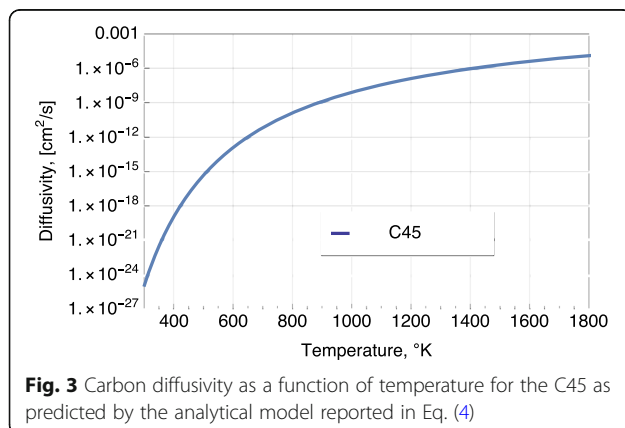
Table 2 Diffusion length evaluated at different temperatures (interaction time 1 s)

Temperature [°C]	(Karabelchtchikova and Sisson Jr 2006) Diffusion length [µm]	(Lee et al. 2011)
880	4.09	0.29
980	2.46	0.77
1080	–	1.69
1180	–	3.24

diffusion, a high spatially resolved indentation technique is necessary. Conventional indentation techniques are not able to satisfy this request, due to the large size of the indenter (compared to the grain structure of the sample). For this purpose, an alternative technique is represented by atomic force microscopy (AFM) equipped with a diamond tip as an indenter and imaging probe at the same time. With this technique, it is possible to select the desired area of the sample and to proceed with indentation directly with the AFM tip, taking advantage of the nanometric spatial resolution typical of this kind of apparatus. The indentation marks can be imaged immediately after using the same indentation tip (Bhushan and Koinkar 1994; Butt et al. 2005). In addition, the use of AFM as indenter allows the application of a smaller load with respect to conventional indention, down to pN values. Such a reduced load generates very small marks and, consequently, high-density indentation matrices, increasing the resolution of the final hardness map. This technique enables the determination of hardness by a direct method, namely calculating the ratio L/A, where L is the applied load and A is the projected area. The alternative and most used indirect method to determine hardness consists of analysing the approach-retract indentation curve (Oliver-Pharr method (Oliver and Pharr 1992)). As already reported in literature (Miyake et al. 2004; Liang and Yao 2007), the Oliver-Pharr indirect method overestimates the hardness, because the generated pile-up cannot be taken into account. Therefore, the use of AFM as hardness tester appears powerful and attractive, both for the spatial resolution and for its sensitivity to pile-up generation. On the other hand, AFM indentation suffers from non-central geometry of the indenter, which induces the in-plane sliding of the tip during indentation (Kempf et al. 1998; Calabri et al. 2007). This effect, together with creep and hysteresis of the piezo-actuators, could introduce a systematic error to the hardness absolute value.

In this study, AFM equipped with a diamond tip was used to generate a high-resolution hardness map of the steel surfaces. The abovementioned drawback related to AFM indentation is not critical for the purpose of the

Fig. 3 Carbon diffusivity as a function of temperature for the C45 as predicted by the analytical model reported in Eq. (4)

present study, where the relative spatial variation and distribution of hardness are the key quantities.

The experimental set-up

In the present work, the negligible austenite homogenization during laser hardening process has been experimentally verified through hardness measurements on C45 specimens laser and oven treated obtained by means of atomic force microscopy (AFM) technique.

Specimens for laser treatments were 155 × 80 × 15 mm in order to guarantee an adequate thermal inertia for the cooling while the samples oven treated were smaller, roughly 30 × 20 × 15, all the material was annealed in oven obtaining pure perlite/ferritic mixture. Oven treated sample was heated at 840 °C for with low and controlled temperature gradient in the oven (austenitization), maintained at this temperature for 3 h (carbon homogenization in austenite) and quenched in water. Laser hardened sample was treated with a EL.EN FAF 3 kW continuous wave CO_2 laser focused at 6 mm, operating at a power between 1100 and 1360 W, and scanning speed between 0.6 and 0.3 m/min resulting in a range of influence between 2.9 and 5.7 kJ/cm^2. For a better coupling between the 10.6 μm wavelength of the CO_2 laser and the material surface, a thin coating of graphite was applied in spray form. During the experiments, the surface under treatment was protected supplied through a lateral nozzle in order to decrease the effects of oxidation.

Given similar overall results for the two treatments, the AFM measurements were conducted on both the oven treated and laser-treated samples (Fig. 4).

The hardness of the laser-exposed region was investigated in a perpendicular cross-section of the sample, at about 24.5 μm from the treated surface to avoid the effects due to surface oxidation (the laser effect is expected to extend at least 1 mm from the surface) (Fig. 4a). For comparison, the pristine hardness was measured in an untreated region of the same sample, at a distance of 10 mm from the exposed surface (Fig. 4b). The analysis of the indentation matrices enables the drawing of the corresponding hardness maps for the laser-treated and untreated regions. For comparison, the same procedure was repeated on a standard heat-tempered sample.

The hardness maps in different regions of the sample (Fig. 4) were obtained by making regular indentation matrices using a Veeco DI-EnviroScope AFM, working in nano-indentation mode. The indenter consisted in a diamond Berkovich tip glued on a sapphire cantilever.

The elastic constant of the cantilever, according to Company calibration, was 5085 N/m and the applied load during indentation was between 1.23 and 1.25 μN. The angle between the cantilever and the surface was
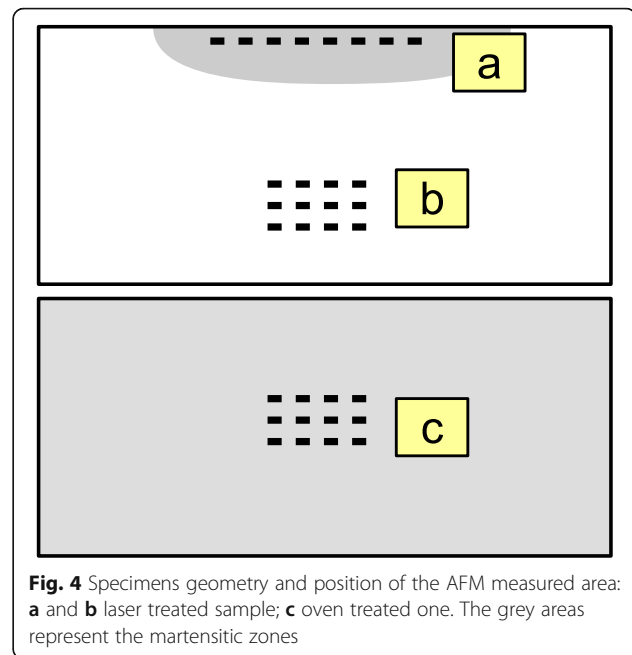

Fig. 4 Specimens geometry and position of the AFM measured area: **a** and **b** laser treated sample; **c** oven treated one. The grey areas represent the martensitic zones

12°. The hardness in each position of the matrix was obtained using the direct method, namely dividing the applied load by the projected area of indentation, measured in tapping mode AFM using the same indentation tip.

The hardness absolute values have been reported, even if, as already discussed, the reliability of AFM indentation is still debated, related to the non-central geometry of the indenter and the hysteresis and creep of the piezo-actuator. Anyway, for the purpose of the present study, the reader must focus on the hardness gradient of the investigated surface and on its distribution rather than on the absolute value.

Results and discussion

Full martensite structures were obtained on the oven treated and in the track of the laser patterned samples with an average HV$_{1000}$ microhardness of 670. A representative image of the section of the patterned track is shown in Fig. 5. No appreciable melted and re-casted phases were observed during the experimental campaign and for the tested conditions.

In Fig. 6a, the AFM image of a typical indentation matrix is reported. As can be seen, the distance among the indentations in the x and y direction is about 2.6 μm. To measure the projected area of each mark, high-resolved AFM images were acquired, so to improve the spatial resolution. The axis length of the triangular projected area is between 300 and 600 nm, while the depth goes from 10 to 100 nm. As an example, in Fig. 6b, the AFM high-resolution magnification of two adjacent indentation marks is reported. The two marks are
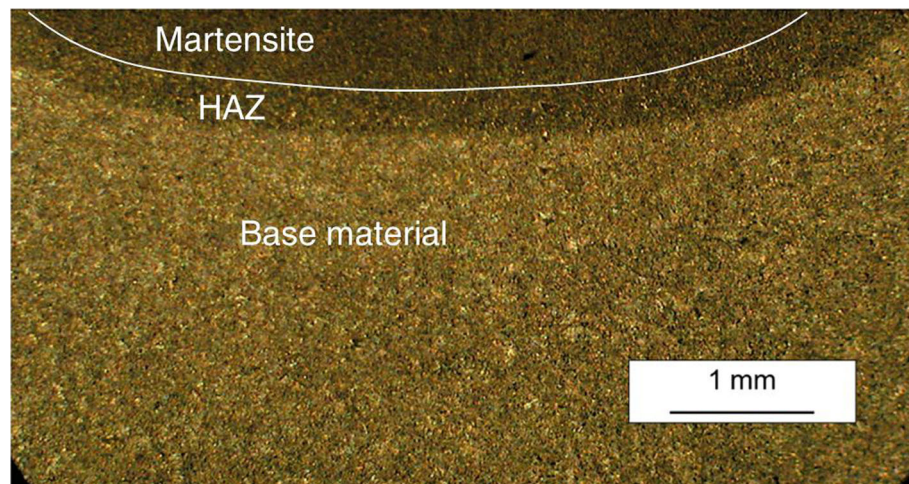
Fig. 5 Section of a laser hardened track. Power = 1.36 kW, scanning speed = 0.6 m/min

characterized by different projected area and depth, evident from the corresponding distance–height graph (Fig. 6c). The measurement of the projected area related to the applied load enables the drawing of the hardness map of the selected region.

In Fig. 7, three different hardness maps are reported, obtained by means of AFM nano-indentations. Figure 7a, b represents the hardness maps in two different regions closed to the laser-treated surface (24.5 μm from the surface) while Fig. 7c is related to a portion of the sample that was not influenced by laser exposure.

The colour scale is the same in all the maps for a better comparison, while the lateral dimensions are different. In both maps, a and b colour spreading is large, corresponding to a hardness variation from 3 to 16 GPa.

Domains of different hardness are recognizable in the maps, with a mean linear grain size between 7 and 9 μm, calculated by a standard self-correlation function. In the map c, which corresponds to the untreated bulk portion of the specimen, the hardness appears almost uniformly distributed between 3 and 7 GPa, and no domains are evident. The hardness domain size in a and b is similar to the mean size of the steel grains. The fact that after laser exposure high-hardness domains appeared with the same dimensions of steel grains indicates that C atoms did not completely diffuse in the material, but remained confined in perlitic grains.

To quantify the statistical distribution of hardness in the tested regions of the specimen, the corresponding histograms are reported in Fig. 8.
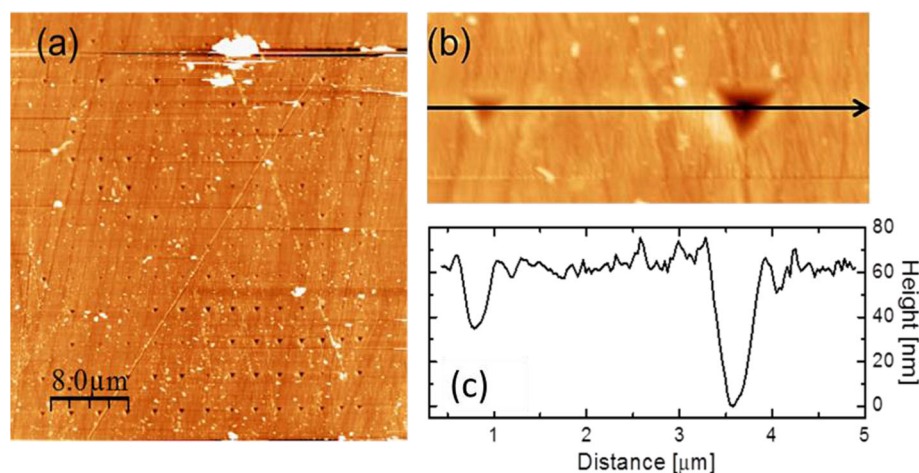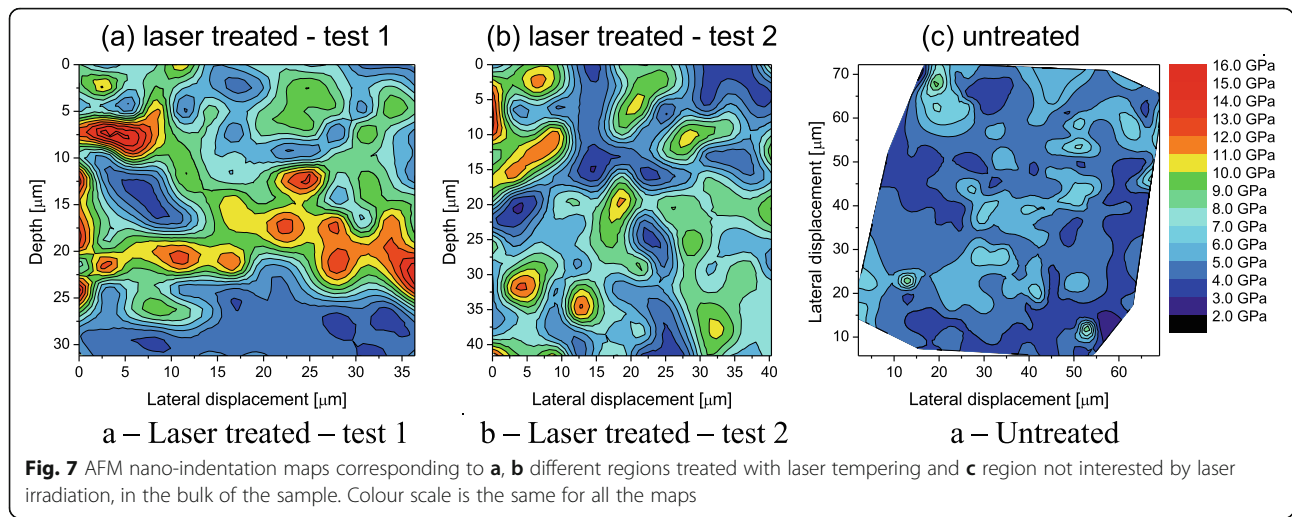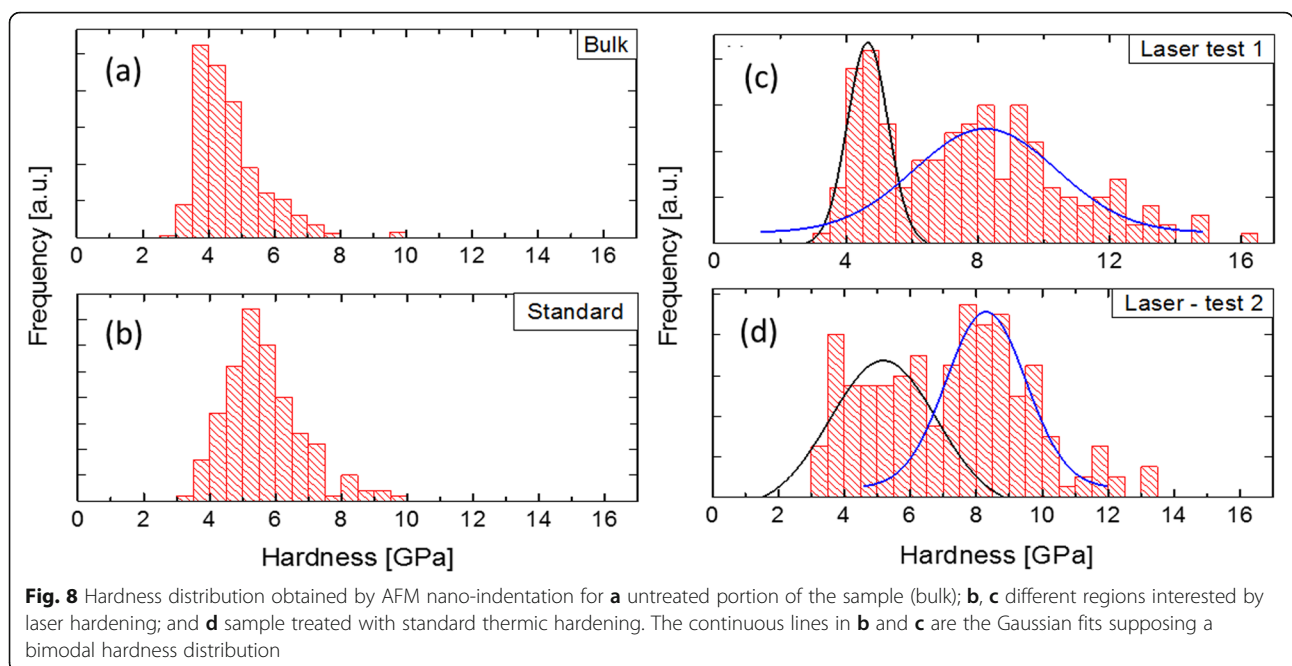

Fig. 6 a AFM image of an indentation matrix on the sample treated with laser hardening with power = 1.36 kW and scanning speed 0.6 m/min; **b** high-resolution AFM image of two neighbouring indentations, used for the estimation of the projected indentation area; and **c** height profile of the indentations reported in **b**

Fig. 7 AFM nano-indentation maps corresponding to **a**, **b** different regions treated with laser tempering and **c** region not interested by laser irradiation, in the bulk of the sample. Colour scale is the same for all the maps

In the histogram in Fig. 8a, which corresponds to the untreated region, the hardness distribution is single-peaked between 3.5 and 5.0 GPa, asymmetric toward larger value (lognormal distribution), confirming the absence of multiple hardness domains. The hardness distributions corresponding to the laser-treated region are significantly different from that of the untreated region (Fig. 8b, c). As already mentioned, the spread of values is very large without observing the presence of a single peak. We can speculate the occurrence of a bimodal distribution in both, with peaks at about 4.5 and 8.3 GPa for histogram a, and 4.7 and 8.4 GPa for histogram b. This thesis is supported by the agreement

between the related Gaussian fits and the corresponding hardness distribution suggesting that part of the treated material undergoes the transformation to austenite, but a relevant portion has the same hardness of the untreated region. This is in good agreement with what proposed in (Orazi et al. 2010; Fortunato et al. 2013) where, due to the short interaction time of laser hardening, C intra-diffusion takes place in the perlite colony, but inter-diffusion and homogenisation of ferrite grains are negligible. Considering the domain size calculated from map a and b, it follows that the C mean diffusion length is not larger than 10 μm. This result is in agreement with previous findings on laser-treated steel analysed by

Fig. 8 Hardness distribution obtained by AFM nano-indentation for **a** untreated portion of the sample (bulk); **b**, **c** different regions interested by laser hardening; and **d** sample treated with standard thermic hardening. The continuous lines in **b** and **c** are the Gaussian fits supposing a bimodal hardness distribution

classical indentation taking into account the large size of the indenter, which reported a progressive decrease of hardness with the distance from the exposed area (Orazi et al. 2010). In Fig. 8d, the hardness distribution of a sample treated with standard tempering is reported. As expected, in this case the distribution is single-peaked, confirming a homogenous diffusion of C in all the austenitic grains. The lower absolute value measured in this case with respect to laser-treated sample is related to the difficulty in maintaining exactly the same set-up parameters (laser alignment on the AFM cantilever) and other systematic error intrinsic to AFM indentation (non-central geometry of the indenter, creep and hysteresis of the piezo-actuators), as briefly discussed in the previous section.

Conclusions

In the present work, a novel simplified approach for laser surface hardening modelling is presented and discussed based on the assumption of neglecting the austenite homogenization during the heating phase of the process. The aim of the work was the experimental validation of this postulation through hardness measurements on C45 specimens laser and oven treated obtained by means of atomic force microscopy (AFM) technique. The achieved uneven AFM nano-indentation maps of laser hardened portions of the specimens indicated that carbon atoms did not completely diffuse in the material but remained confined in the perlitic grains. A hardness spread of 13 GPa was acquire for the laser-treated regions, significantly greater than the 4 GPa of the untreated region. A statistical elaboration of the acquired data showed a bimodal hardness distribution of the laser hardened portions once more suggesting that only a part of the treated material transformed to austenite homogenized its carbon content; this could moreover explain the slightly higher hardness of the laser hardened material compared to heat-treated one.

Abbreviations
AFM: Atomic force microscopy; BCC: Body-centred cubic; FCC: Face-centred cubic

Acknowledgements
Not applicable

Authors' contributions
Leonardo Orazi: L.O., Alberto Rota A.R., Barbara Reggiani B.R. L.O. and A.R. were involved in planning and supervised the work. L.O., A.R. and B.R. processed the experimental data, performed the analysis, drafted the manuscript and designed the figures. L.O., A.R. performed the hardness and AFM measurements. All authors aided in interpreting the results, worked on the manuscript, discussed the results and commented on the manuscript. The authors read and approved the final manuscript.

Funding
No founding have been received for this research.

Author details
[1]DISMI - Department of Sciences and Methods for Engineering, University of Modena and Reggio Emilia, Reggio Emilia, Italy. [2]EN&TEC - Centro Interdipartimentale per la Ricerca Industriale ed il Trasferimento Tecnologico nel Settore delle Tecnologie Integrate per la Ricerca Sostenibile, della Conversione Efficiente dell'Energia, l'Efficienza Energetica degli Edifici, l'Illuminazione e la Domotica, University of Modena and Reggio Emilia, Reggio Emilia, Italy. [3]FIM – Department of Physics, Informatics and Mathematics, University of Modena and Reggio Emilia, Modena, Italy. [4]INTE RMECH - Centro Interdipartimentale per la Ricerca Applicata e i Servizi nel settore della Meccanica Avanzata e della Motoristica, University of Modena and Reggio Emilia, Modena, Italy.

References
Ashby, M. F., & Easterling, K. E. (1984). The transformation hardening of steel surfaces by laser beam - hypo-eutectoid steels. *Acta Metallurgica*, 32(11), 1935–1948.

Babu, P. D., Buvanashekaran, G., & Balasubramanian, K. R. (2013). Experimental investigation of laser transformation hardening of low alloy steel using response surface methodology. *Int J Adv Manuf Technol*, 67(5), 1883–1897.

Babu, P. D., & Marimuthu, P. (2019). Status of laser transformation hardening of steel and its alloys: a review. *Emerging Materials Research*, 8(2), 188–205.

Bhadesia, H. K. D. H. (1981). Diffusion of carbon in austenite. *Metal Science*, 15, 477–479.

Bhushan, B., & Koinkar, V. N. (1994). Nanoindentation hardness measurements using atomic force microscopy. *Applied Physics Letters*, 64(13), 1653–1655.

Butt, H. J., Cappella, B., & Kappl, M. (2005). Force measurements with the atomic force microscope: Technique, interpretation and applications. *Surface Science Reports*, 59(1–6), 1–152.

Calabri, L., Pugno, N., Rota, A., Marchetto, D., & Valeri, S. (2007). Nanoindentation shape effect: experiments, simulations and modelling. *Journal of Physics: Condensed Matter*, 19(39), 395002.

Chen, C., Zeng, X., Wang, Q., Lian, G., & YanWang, X. H. (2020). Statistical modelling and optimization of microhardness transition through depth of laser surface hardened AISI 1045 carbon steel. *Optics & Laser Technology*, 124, 105976.

Fortunato, A., Ascari, A., Liverani, E., Orazi, L., & Cuccolini, G. (2013). A comprehensive model for laser hardening of carbon steels. *Journal of Manufacturing Science and Engineering*, 135, 1–8 2013.

Furuhara, T., Yamaguchi, J., Sugita, N., Miyamoto, G., & Maki, T. (2003). Nucleation of proeutectoid ferrite on complex precipitates in austenite. *ISIJ International*, 43(10), 1630–1639.

Ion, J. C. (2002). Laser transformation hardening. *Surface Engineering*, 18(1), 14–31.

Jacot, A., & Rappaz, M. (1997). A two-dimensional diffusion model for the prediction of phase transformation: application to austenization and homogenization of hypoeutectoid fe-c steels. *Acta mater.*, 45(2), 575–585.

Jacot, A., & Rappaz, M. (1998). Modeling of reaustenization from the perlite structure in steel. *Acta mater.*, 46(11), 3949–3962.

Karabelchtchikova, O., & Sisson Jr., R. D. (2006). Carbon diffusion in steels: a numerical analysis based on direct integration of the flux. *Journal of Phase Equilibria and Diffusion*, 27, 598–604.

Kempf, M., Göken, M., & Vehoff, H. (1998). Nanohardness measurements for studying local mechanical properties of metals. *Applied Physics A*, 66, S843–S846.

Lee, S.-J., Matlock, D. K., & Van Tyne, C. J. (2011). An empirical modelfor carbon diffusion in austenite incorporating alloying element effects. *ISIJ International*, 51(11), 1903–1911.

Li, W. B., Easterling, K. E., & Ashby, M. F. (1986). The transformation hardening of steel surfaces by laser - ii hypereutectoid steels. *Acta Metallurgica*, 34(8), 1533–1543.

Liang Zhou and Yingxue Yao. (2007) Single crystal bulk material micro/nano indentation hardness testing by nanoindentation instrument and afm. *Materials Science and Engineering: A, 460–461*(0), 95 – 100.

Miokovic, T., Schulze, V., Vhringer, O., & Lhe, D. (2006). Prediction of phase transformation during laser surface hardening of aisi 4140 including the effects of inhomogeneus austenite formation. *Materials Science and Engineering A, 435-436*, 547–555.

Miokovic, T., Schulze, V., Vhringer, O., & Lhe, D. (2007). Influence of cyclic temperature changes on the microstructure of aisi 4140 after laser surface hardening. *Acta Materialia, 55*, 589–288 599.

Miyake, K., Fujisawa, S., Korenaga, A., Ishida, T., & Sasaki, S. (2004). The effect of pile-up and contact area on hardness test by nanoindentation. *Japanese Journal of Applied Physics, 43*(7B), 4602–4605.

Mühl, F., Jarms, J., Kaiser, D., Dietrich, S., & Schulze, V. (2020). Tailored bainitic-martensitic microstructures by means of inductive surface hardening for AISI4140. *Materials and Design, 195*, 108964.

Ohmura, E., & Inoue, K. (1989). Computer simulation on structural changes of hypoeutectoid steel in laser transformation hardening process. *JSME International Journal, 32*, 45–53.

Oliver, W. C., & Pharr, G. M. (1992). An improved technique for determining hardness and elastic modulus using load and displacement sensing indentation experiments. *Journal of Materials Research, 7*, 1564–1583 5.

Orazi, L., Fortunato, A., Cuccolini, G., & Tani, G. (2010). An efficient model for laser surface hardening of hypo-eutectoid steels. *Applied Surface Science, 256*(6), 1913–1919.

Patwa, R., & Shin, Y. C. (2006). Predictive modeling of laser hardening of aisi5150h steels. *International Journal of Machine Tools & Manufacture, 46*, 3949–3962.

Skvarenina, S., & Shin, Y. C. (2006). Predictive modeling and experimental results for laser hardening of aisi 1536 steel with complex geometric features by a high power diode laser. *Surface & Coatings Technology, 46*, 3949–3962.

Smith, R. P. (1953). The diffusivity of carbon in iron by the steadystate method. *Acta Metallurgica, 1*(5), 578–587.

Tani, G., Fortunato, A., Ascari, A., & Campana, G. (2010). Laser surface hardening of martensitic stainless steel hollow parts. *CIRP Annals - Manufacturing Technology, 59*(1), 207–210.

Tani, G., Orazi, L., & Fortunato, A. (2008). Prediction of hypo eutectoid steel softening due to tempering phenomena in laser surface hardening. *CIRP Ann Manuf Technol, 57*(1), 209–212.

Tibbetts, G. G. (1980). Diffusivity of carbon in iron and steels at high temperatures. *Journal of Applied Physics, 51*(9), 4813–4816.

Weels, C., Batz, W., & Mehl, R. F. (1950). Diffusion coefficient of carbon in austenite. *Trans. AIME, 188*, 553–560.

Weels, C., & Mehl, R. F. (1940). Rate of diffusion of carbon in austenite in plain carbon, in nickel and in manganese steels. *Trans. AIME, 140*, 279–306.

Publisher's Note